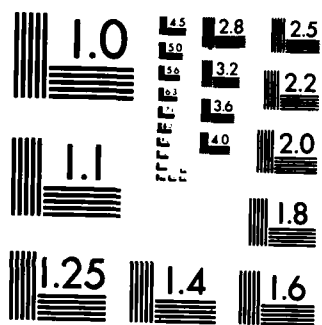


AD-A147 528 SWIR AND VISIBLE ATOMIC EMISSION FROM LASER-PRODUCED 1/1
OXYGEN AND NITROGEN PLASMAS(U) AIR FORCE GEOPHYSICS LAB
HANSCOM AFB MA J B LURIE ET AL. 15 JUN 84
UNCLASSIFIED AFGL-TR-84-0161 F/G 17/5 NL





12

AFGL-TR-84-0161
ENVIRONMENTAL RESEARCH PAPERS, NO. 882

AD-A147 528

SWIR and Visible Atomic Emission From Laser-Produced Oxygen and Nitrogen Plasmas

JONATHAN B. LURIE
STEVEN M. MILLER
RUSSELL A. ARMSTRONG



15 June 1984

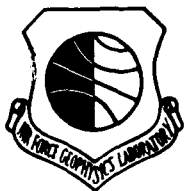


Approved for public release; distribution unlimited.



DTIC
ELECTE
NOV 14 1984
S E D

DTIC FILE COPY



INFRARED TECHNOLOGY DIVISION

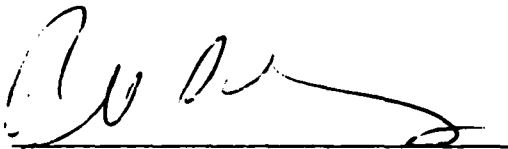
PROJECT 2310

AIR FORCE GEOPHYSICS LABORATORY

HANSCOM AFB, MA 01731

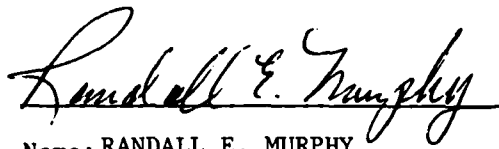
84 11 05 086

"This technical report has been reviewed and is approved for publication"



Name: RUSSELL A. ARMSTRONG
Branch Chief

FOR THE COMMANDER



Name: RANDALL E. MURPHY
Division Director

This report has been reviewed by the ESD Public Affairs Office (PA) and is releasable to the National Technical Information Service (NTIS).

Qualified requestors may obtain additional copies from the Defense Technical Information Center. All others should apply to the National Technical Information Service

If your address has changed, or if you wish to be removed from the mailing list, or if the addressee is no longer employed by your organization, please notify AFGL/DAA, Hanscom AFB, MA 01731. This will assist us in maintaining a current mailing list.

Do not return copies of this report unless contractual obligations or notices on a specific document requires that it be returned.

UNCLASSIFIED

SECURITY CLASSIFICATION OF THIS PAGE

REPORT DOCUMENTATION PAGE				
1a. REPORT SECURITY CLASSIFICATION UNCLASSIFIED		1b. RESTRICTIVE MARKINGS		
2a. SECURITY CLASSIFICATION AUTHORITY		3. DISTRIBUTION/AVAILABILITY OF REPORT Approved for public release; distribution unlimited		
2b. DECLASSIFICATION/DOWNGRADING SCHEDULE				
4. PERFORMING ORGANIZATION REPORT NUMBER(S) AFGL-TR-84-0161 ERP, No. 882		5. MONITORING ORGANIZATION REPORT NUMBER(S)		
6a. NAME OF PERFORMING ORGANIZATION Air Force Geophysics Laboratory	6b. OFFICE SYMBOL (If applicable) LSI	7a. NAME OF MONITORING ORGANIZATION		
6c. ADDRESS (City, State and ZIP Code) Hanscom AFB Massachusetts 01731		7b. ADDRESS (City, State and ZIP Code)		
8a. NAME OF FUNDING/SPONSORING ORGANIZATION	8b. OFFICE SYMBOL (If applicable)	9. PROCUREMENT INSTRUMENT IDENTIFICATION NUMBER		
8c. ADDRESS (City, State and ZIP Code)		10. SOURCE OF FUNDING NOS.		
		PROGRAM ELEMENT NO.	PROJECT NO.	TASK NO.
		61102F	2310	G4
11. TITLE (Include Security Classification) SWIR and Visible Atomic Emission from Laser-Produced Oxygen		14. DATE OF REPORT (Yr., Mo., Day) 1984 June 15		
12. PERSONAL AUTHOR(S) and Nitrogen Plasmas Lurie, Jonathan B., Miller, Steven M., Armstrong, Russell A.		15. PAGE COUNT 19		
13a. TYPE OF REPORT Scientific Interim	13b. TIME COVERED FROM N/A TO			
16. SUPPLEMENTARY NOTATION				
17. COSATI CODES		18. SUBJECT TERMS (Continue on reverse if necessary and identify by block number)		
FIELD	GROUP	SUB GR.		
04	01			
		Infrared Laser Breakdown Laser Plasma Rydberg States		
19. ABSTRACT (Continue on reverse if necessary and identify by block number) We report the first observations of structured infrared emission from atomic Rydberg states produced by three-body recombination of laser-produced oxygen and nitrogen plasmas. Emission is observed in the 2.00 to 3.25 μ spectral region through the use of a simple grating monochromator. In addition, we discuss time-resolved visible emission studies that provide temporal information on the atomic infrared-emitting states. Implications are considered for the observation of LWIR emission from higher Rydberg levels.				
20. DISTRIBUTION/AVAILABILITY OF ABSTRACT UNCLASSIFIED/UNLIMITED <input checked="" type="checkbox"/> SAME AS RPT <input type="checkbox"/> DTIC USERS <input type="checkbox"/>		21. ABSTRACT SECURITY CLASSIFICATION UNCLASSIFIED		
22a. NAME OF RESPONSIBLE INDIVIDUAL JONATHAN B. LURIE		22b. TELEPHONE NUMBER (Include Area Code) (617) 861-3671	22c. OFFICE SYMBOL LSI	

DD FORM 1473, 83 APR

EDITION OF 1 JAN 73 IS OBSOLETE

UNCLASSIFIED

SECURITY CLASSIFICATION OF THIS PAGE

Preface

We thank Drs. W. Blumberg, R. Stachnik, and W. Rawlins for helpful suggestions and the loan of the InSb detector. This research was supported by AFOSR, Task 2310G4, and DNA.

Accession For	
NTIS GRA&I	<input checked="" type="checkbox"/>
DTIC TAB	<input type="checkbox"/>
Unannounced	<input type="checkbox"/>
Justification	
By _____	
Distribution/	
Availability Codes	
Dist	Avail and/or Special
A-1	



Contents

1. INTRODUCTION	7
2. EXPERIMENTAL	8
3. RESULTS	10
4. DISCUSSION	14
5. CONCLUSION	18
REFERENCES	19

Illustrations

1. Experimental Apparatus for LINUS Infrared Emission Studies	9
2. Experimental Apparatus for LINUS Time-Resolved Visible Emission Studies	10
3. Emission Spectrum of Laser-Produced Oxygen Plasma from 2.00 to 3.25 μ	11
4. Emission Spectrum of Laser-Produced Nitrogen Plasma from 2.00 to 3.25 μ	12
5. Time-Resolved Emission Spectra of Laser-Produced Oxygen Plasma from 610 to 620 nm	13

Tables

1. Assignments of Observed Atomic Infrared Lines	12
2. Emission Times-to-Peak and Exponential Fall Times of Nitrogen Ion Lines	14

SWIR and Visible Atomic Emission From Laser-Produced Oxygen and Nitrogen Plasmas

1. INTRODUCTION

We have been interested for some time in the inter-Rydberg level transitions resulting from a recombining plasma that give rise to infrared (IR) emission. Models predicting the IR emission from such a process have been developed based on known or calculated energy levels, and on assuming a Coulomb attraction potential for the calculation of intensity functions.¹ Such calculations are taken to be quite reasonable, especially for oxygen (O) and nitrogen (N), which are strictly L-S coupled. Production mechanisms for excited states are less certain, and statistical and/or cascade behavior is generally accepted as a basis for population arguments.² Deviation from assumed behavior can lead to errors in predictions of IR spectral emission models. Therefore, benchmark measurements of IR emission from a recombining plasma would be quite useful. Early observations³ of electron-excited air at 160 Torr and O₂ and N₂ in a hollow-cathode

(Received for publication 13 June 1984)

1. Sappenfield, D. (1981) Radiation from a Recombining Oxygen Plasma, Los Alamos Supplemental Report LA-4303.
2. Rawlins, W. T., Gelb, A., and Armstrong, R. A. (1983) COCHISE Observations of Argon Rydberg emission from 2-16 μ m, AFGL-TR-83-0201, AD A137916.
3. Murphy, R. W., Fairbairn, A. R., Rogers, W. J., and Hart, A. M. (1975) Near IR nuclear spectra: Interpretation by recent laboratory results, Fourth DARPA Strategic Space Symposium, 23 September 1975.

discharge tube identified certain SWIR transitions that were likely produced by direct electron impact, although plasma relaxation may have accounted for some of the hollow cathode emission.

The investigation of the relaxation of laser-produced O_2 and N_2 high-temperature plasmas at low pressure (10 to 30 Torr) has been the focus of our Laser-Induced Nuclear Simulation (LINUS) program. Until this time, the primary emphasis of these experiments has been the characterization of the laser-produced plasma through the use of visible emission spectroscopy. Specifically, observations of visible emission from O_2 and N_2 plasmas yielded information on which species were produced and their temporal behavior.⁴ In addition, studies on helium (He) produced data on electron temperatures and densities as a function of time.⁵ Although these experiments have produced much useful information concerning the physics and chemistry of the plasma, and therefore, what might be observed in the IR, no direct observations of the IR emission from these plasmas have been obtained.

In this report, we present observations of visible and SWIR emission from laser-produced O_2 and N_2 plasmas. The line emission observed in the SWIR originates from high-lying atomic states generated by ion-electron recombination. We discuss time-resolved visible emission studies that provide additional information on the behavior of important atomic IR-emitting states. In addition, implications are drawn for the observation of LWIR emission from very high-lying atomic Rydberg states.

2. EXPERIMENTAL

Figure 1 illustrates the experimental apparatus used for the IR emission studies. A Quanta-Ray Nd:YAG laser (model DCR-1A, $\lambda = 1.064 \mu$, 10 nsec FWHM multilongitudinal mode pulse, 10-Hz repetition rate) was focussed with a 51-mm f.l. biconvex lens into a gas cell containing O_2 or N_2 . The laser was propagated parallel to the monochromator entrance slit. The windows on the cell and all emission focusing optics were manufactured from calcium fluoride (CaF_2). A typical average laser power of 4 W created an intensity of $2 \times 10^{13} \text{ W/cm}^2$ in the focal region.

The radiation from the laser-produced plasma was collected at 90° to the axis of the laser beam and collimated using a 100-mm f.l. lens. In order to

4. Armstrong, R.A., Lucht, R.A., and Rawlins, W.T. (1983) Spectroscopic investigation of laser-initiated low-pressure plasmas in atmospheric gases, *Appl. Opt.* 22:1573.

5. Lurie, J.B., and Bashkin, S., to be published.

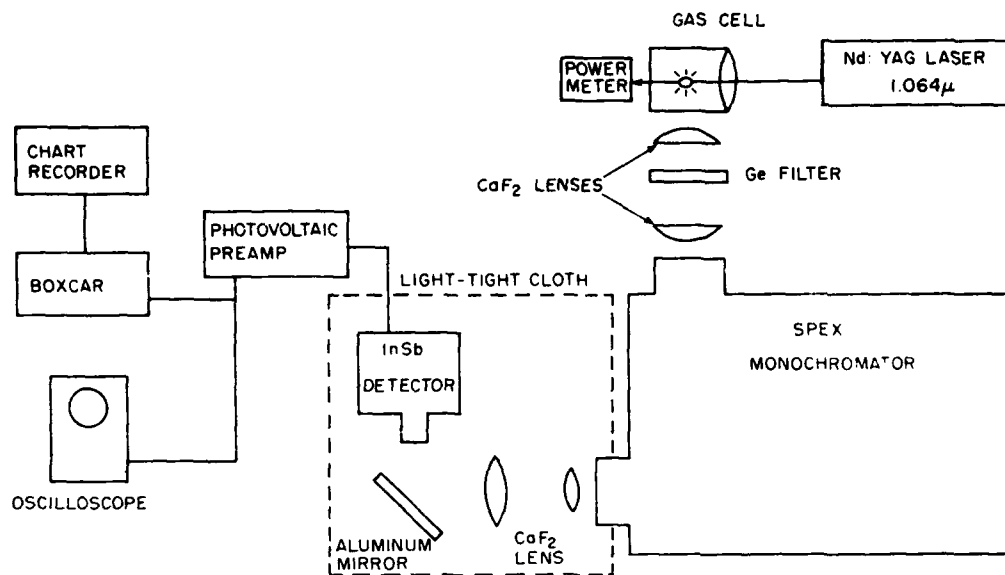


Figure 1. Experimental Apparatus for LINUS Infrared Emission Studies

prevent scattered laser radiation and visible and UV plasma emission from reaching the detector, a germanium (Ge) long-pass filter was used. This blocked wavelengths $< 1.8 \mu$. The IR plasma emission was focused onto the entrance slit of a Spex 1870 monochromator (0.5 m f.l.) using a 100-mm f.l. lens, which slightly overfilled the 300 lines/mm grating. The grating was blazed at 3.0μ . The emission passing through the exit slit was collected and collimated using a 75-mm f.l. lens and turning mirror. The detector was an SBRC model E348 InSb photovoltaic device contained in an SBR model 44782 metal dewar. The signal from the detector was amplified using an SBRC A220 preamplifier. Signal processing was done with a PAR 162-165 boxcar averager using a 50-nsec gate. The output of the boxcar was recorded on a strip chart recorder.

The collection optics and detector were entirely enclosed by a light-tight black cloth to eliminate visible and near-IR radiation, except for the signal passing through the monochromator.

Figure 2 illustrates the apparatus used for the collection of time-resolved visible emission spectra. The spectrometer was fitted with a PAR OMA II (optical multichannel analyzer) in place of the exit slit, and a 1200 grooves/mm grating blazed at 5000 \AA . This arrangement provided spectral resolution of $\sim 2 \text{ \AA}$. Each time-resolved spectrum was recorded by letting emission intensity build up on the cooled silicon intensified detector (SIT) for 500 detector electron beam scans, and then recording the signal into memory for 500 scans. A

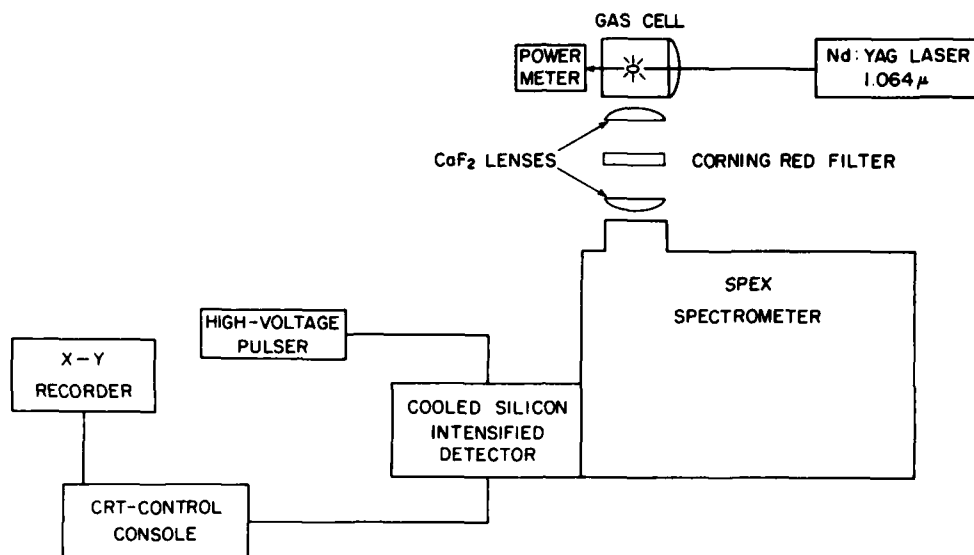


Figure 2. Experimental Apparatus for LINUS Time-Resolved Visible Emission Studies

keystroke routine was written to perform this sequence for the initial setting of the 300-nsec time gate, and advance the time gate and sequence repetition. Using this sequence, a set of nine time-resolved spectra could be recorded in 15 min. The data were stored on floppy disc and subsequently plotted on an X-Y recorder. For these spectra, the laser was propagated perpendicular to the monochromator entrance slit and focused into the gas cell with a 65-mm plano-convex lens. The gases used were research-grade Matheson.

3. RESULTS

Figures 3 and 4 illustrate time-integrated emission spectra for 20 Torr O_2 and N_2 plasmas in the 2.00 to 3.25 μ region with spectral resolution of 0.02 μ . The emission lifetimes as observed on an oscilloscope are $\sim 2 \mu\text{sec}$, which is roughly the time response of the detector-preamplifier combination. The spectra clearly exhibit scattered 1.064- μ laser radiation in second and third order. The continuum features of both spectra exhibit roughly similar overall contours, both showing absorption in the 2.6 to 2.8 μ region (H_2O). The O_2 spectrum contains line radiation at 2.65, 2.76, and 2.89 μ and a broad feature centered at 3.09 μ , while the N_2 spectrum contains weaker structured features at 2.92 and

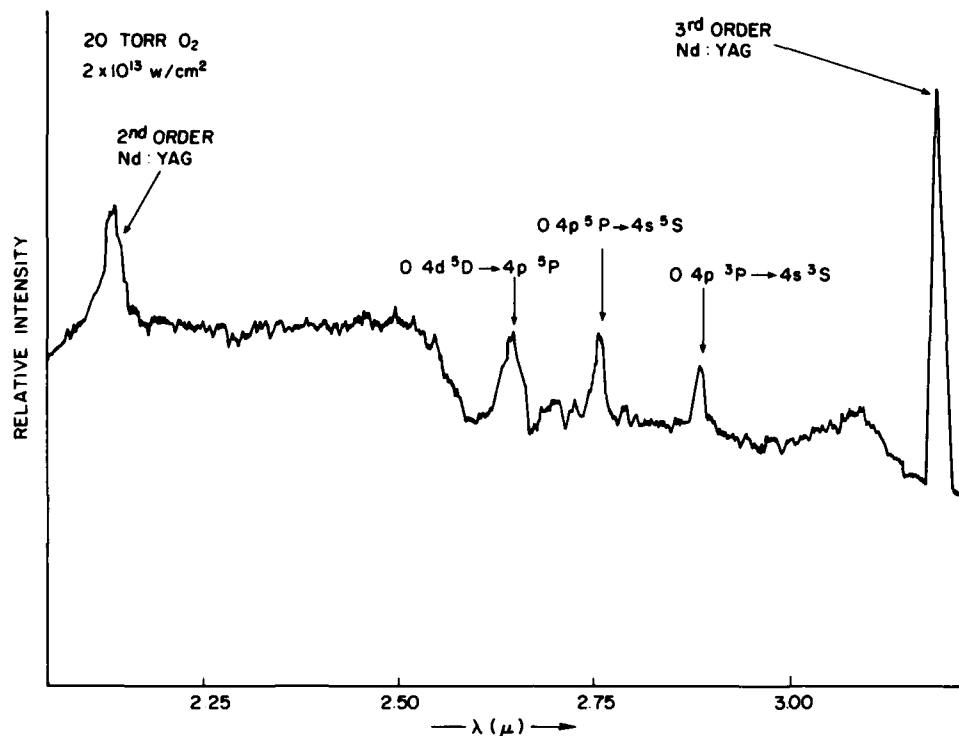


Figure 3. Emission Spectrum of Laser-Produced Oxygen Plasma from 2.00 to 3.25 μ

3.02 μ , with a broad feature centered at 3.07 μ . Line assignments are listed in Table 1.⁶ The resolution in these spectra is too low to resolve lines originating in different J-levels of the atomic upper-state manifolds. At this time we cannot positively assign the 3.09- μ feature in O_2 or the 3.07- μ feature in N_2 .

The relatively slow time response of the InSb detector preamplifier combination precludes temporal discrimination between the continuum and line emission. The continuum radiation due to bremsstrahlung and radiative recombination processes is expected to be significant for times less than 300 nsec (see the following OMA data), while the line radiation due to atomic inter-Rydberg level IR transitions should occur on a microsecond-to-millisecond time scale. Use of a state-of-the-science HgCdTe detector (10-nsec time response) is necessary to obtain time-resolved spectra up to the microsecond time regime.

6. Biemont, E., and Grevesse, N. (1973) Infrared wavelengths and transition probabilities for atoms, $3 \leq Z \leq 20$, Atomic Data and Nuclear Data Tables 12:217.

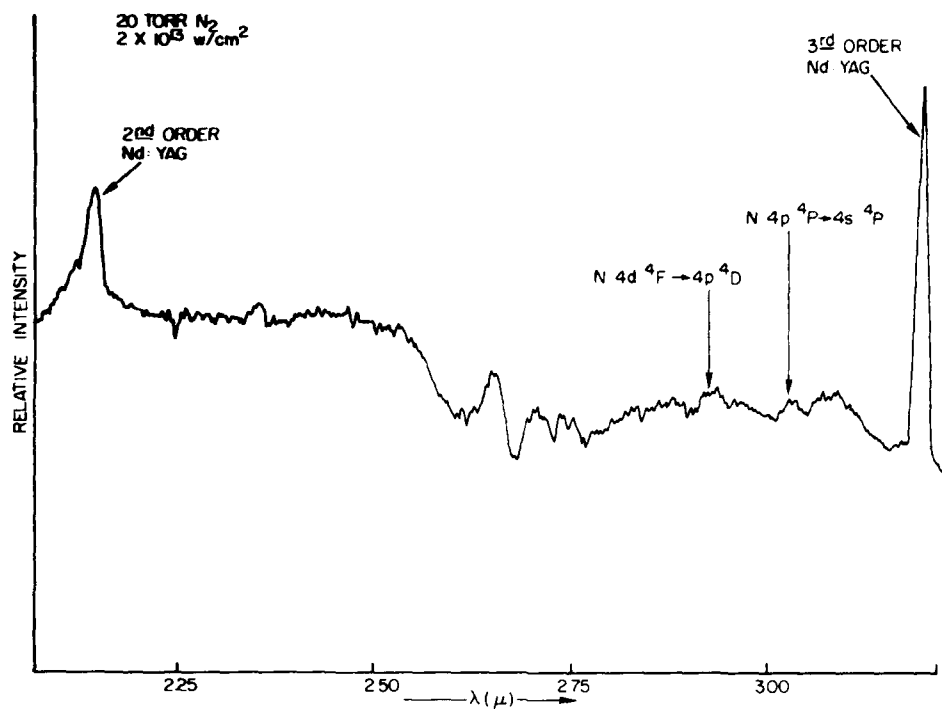


Figure 4. Emission Spectrum of Laser-Produced Nitrogen Plasma from 2.00 to 3.25 μ

Table 1. Assignments of Observed Atomic Infrared Lines

Species	$\lambda (\mu)$	Upper State	Lower State
O	2.65	$4d \ 5D$	$4p \ 5P$
	2.76	$4p \ 5P$	$4s \ 5S$
	2.89	$4p \ 3P$	$4s \ 3S$
N	2.92	$4d \ 4F$	$4p \ 4D$
	3.02	$4p \ 4P$	$4s \ 4P$

Figure 5 illustrates the temporal evolution of the O-atom 6157 Å line. The OMA provides a temporal history of the entire line, recording wavelength on the x-axis, intensity on the y-axis, and relative time on the z-axis. The state giving rise to this emission is the same state that emits the 2.65 μ radiation, 4d⁵D. The time-resolved spectra exhibit several interesting features. First, there is little or no line emission for the first 300 nsec. Instead, a continuum is present due to radiative recombination and bremsstrahlung events. The apparent reduction of the continuum at the edges of the scan is due to the fall-off of the detector array response at its edges. In addition, the emission line exhibits Stark-broadening at early times, which decreases with time as the electron density of the plasma decreases. Although the radiative lifetime of this transition is only 143 nsec,⁷ the peak intensity is not reached until ~1 μsec. This is in sharp contrast to the temporal history of the O⁺ lines,⁴ which show rise times of tens of nanoseconds. While the decay time of the 6157 Å line is ~2 μsec once the peak intensity is reached, the ionic lines decay in hundreds of nanoseconds.⁴ At high

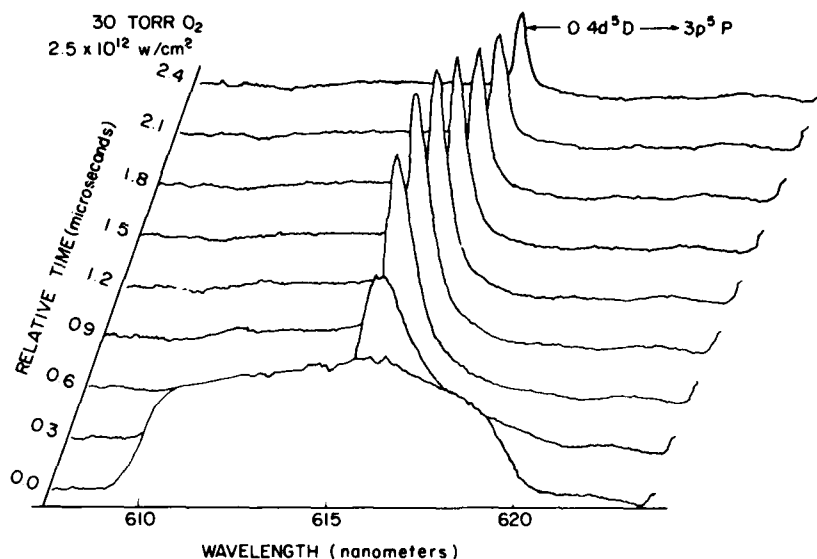


Figure 5. Time-Resolved Emission Spectra of Laser-Produced Oxygen Plasma from 610 to 620 nm

7. Wiese, W.L., Smith, M.W., and Glennon, B.M. (1966) Atomic Transition Probabilities: Volume I, Hydrogen Through Neon, National Standard Reference Data Series - NBS 4.

resolution, the 6157 Å line would appear to be a triplet, in the absence of Stark-broadening of each of the component lines. The relatively low spectral resolution of the OMA, when used with a 1200 grooves/mm grating (~ 2 Å), precludes the observation of the individual lines from the various J-levels, thus determinations of electron temperature and density are not possible from this measurement.

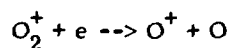
4. DISCUSSION

The data presented by Armstrong, Lucht, and Rawlins⁴ describe almost exclusively ionic transitions in the recombining laser-produced plasma. Their emission times-to-peak and exponential fall times for N ions in a 10 Torr laser-produced N₂ plasma are listed in Table 2. These data suggest strongly that the ions are produced by successive recombination, $N^{3+} \rightarrow N^{2+} \rightarrow N^+$. The data presented in this report are significant for two reasons. First, they show that the ions produced by recombination at early times themselves recombine with electrons to produce highly excited atomic states that emit visible and IR radiation. In addition, these data represent the first observations of spectrally structured IR emission from a highly (at least triply) ionized recombining plasma.

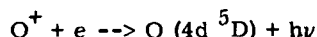
Table 2. Emission Times-to-Peak and Exponential Fall Times of Nitrogen Ion Lines⁴

Line	Time-to-Peak (nsec)	Exponential Fall Time (nsec)
N ³⁺ 3478.7 Å	40	21
N ²⁺ 3938.5 Å	45	37
N ⁺ 4040.9 Å	80	77

The results on the 6157 Å and 2.65 μ O-atom lines are particularly informative since these lines both originate in the 4d ⁵D state. The OMA data illustrate graphically the continuum emission at early times, during which ionic emission is still important, the slow rise (~ 1 μsec) due to ion-electron recombination, and the eventual disappearance of the atomic emission. The process



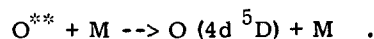
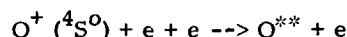
is expected to occur⁸ at a rate of $\sim 10^{-7}$ cm³/sec, although the rate will depend on electron temperature. Time-resolved linewidth data taken in a 200 Torr He laser-produced plasma⁴ indicated an electron density of 1.2×10^{17} /cm³ and an electron temperature of $\sim 50,000$ K for $t=100$ nsec after the laser pulse. Although the He results cannot be applied directly to electron densities and temperatures in the O₂ plasma, nascent electron densities might be expected to be even higher than in the He case since the ionization potentials of O (both molecular and atomic) are considerably lower than that of He. If this is true, then the lifetime of O₂⁺ (X) is expected to be extremely short, and almost certainly cannot account for the long-lived production of the O-atom 4d ⁵D state. The two-body radiative recombination process



is expected to dominate over three-body recombination only when⁹

$$n_e < 1.3 \times 10^{-3} T^4 .$$

We do not expect this condition to apply in the LINUS experiment. Therefore, we favor the process



The ionization potential of atomic oxygen is 109837 cm⁻¹.⁷ In order for the 4d ⁵D state at 102865 cm⁻¹ to be formed directly by recombination, the second electron would have to carry off 0.86 eV in translational energy, an unlikely possibility. Infrared line positions and oscillator strengths calculated using the Coulomb approximation have been tabulated for O and N atoms by Biemont and Grevesse.⁶ Their theoretical results indicate no radiative transitions that would efficiently populate the 4d ⁵D state. In all probability, the 4d ⁵D state is formed by collisional de-excitation of a higher-lying nascent state.

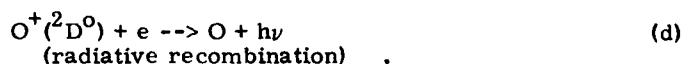
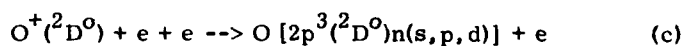
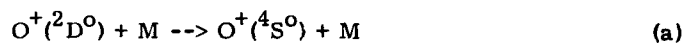
8. Bardsley, J.N., and Biondi, M.A. (1970) in Advances in Atomic and Molecular Physics, D.R. Bates (Ed.) Academic, N.Y., Vol. 6, pp. 1-57.

9. Zel'dovich, Ya., and Raizer, Yu. (1966) Physics of Shock Waves and High-Temperature Hydrodynamic Phenomena, Academic Press, N.Y., p. 405.

The 6157 Å and 2.65 μ data together indicate how it is possible to study the behavior of an important IR-emitting atomic state by observing visible emission from the same state. The time-resolved data acquired by the OMA are much more difficult to collect in the IR.

It is not clear at this time whether the O-atom 4p ⁵P state giving rise to the 2.76 μ emission is created primarily by radiative cascade (4d ⁵D --> 4p ⁵P, λ = 2.65 μ) or by collisional quenching from another Rydberg state. A similar argument applies to the emission at 2.89 μ resulting from the 4p ³P state. The N-atom states observed in IR emission, 4p ⁴P and 4d ⁴F, lie respectively 107037 and 110200 cm⁻¹ above the ground state.¹⁰ The ionization potential of the N atom is 117214 cm⁻¹.⁷ Therefore, the production mechanism of the observed N-atom states is probably similar to that of the O-atom 4d ⁵D state, three-body recombination followed by collisional deactivation of the nascent state. The N-atom states appear to be produced less efficiently than the O-atom states. This is reasonable in view of the higher ionization potential of N.

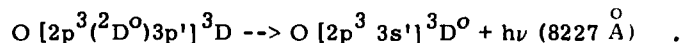
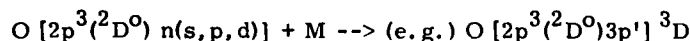
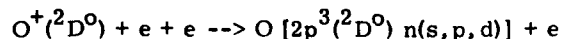
The atomic oxygen states observed here by IR emission can originate only by recombination of O⁺(⁴S^o) with electrons. However, the metastable species O⁺(²D^o) and O⁺(²P^o), lying respectively 136653 cm⁻¹ and 150303 cm⁻¹ above ground state O(³P), are also present. Possible deactivation pathways for these states include:



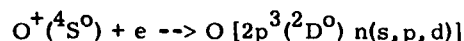
Atomic oxygen states of the configuration described in Reaction (c) lie above the O-atom ionization potential. We have observed visible emission from such states. However, the states from which visible emission has been observed lie < 114,000 cm⁻¹ above the ground state, making direct production by three-body recombination of O⁺(²D^o) unlikely, since the third electron would have to carry away nearly 3 eV of energy. By analogy with the production mechanism

10. Moore, C.E. (1949) Atomic Energy Levels as Derived from the Analyses of Optical Spectra, NBS Circular 467, 15 June 1949.

suggested for the $4d\ ^5D$ state, emission for which $O^+(^2D^0)$ is the precursor is controlled by the processes



The dielectronic recombination process



is another possible production process for atomic oxygen states lying above the ionization energy. However, the discussion by Bates¹¹ suggests that the only such state that could be produced by dielectronic recombination is the $O[2p^3(^2D^0)]3p\ ^3F$ state at $113719\ \text{cm}^{-1}$. While this state is observed in emission at $7950\ \overset{\circ}{A}$,¹¹ other states lying above the ionization energy are observed in our experiment as well. This argues against the contribution of dielectronic recombination to the visible atomic emission in the LINUS studies. Furthermore, Bates¹¹ maintains that dielectronic recombination for $O^+(^4S^0)$ is much slower than radiative recombination. In our IR emission studies we have not observed any O-atom states with a $O^+(^2D^0)$ core configuration.

The IR lines that have been observed in this experiment originate in $n = 4$ for both O and N atoms. These lines have also been observed in low-pressure dc discharges by Saum and Benesch.^{12, 13} Inspection of the calculated line positions and oscillator strengths indicates that LWIR lines of similar oscillator strength to those lines observed in the SWIR might be assigned as the $6d\ ^5D \rightarrow 6p\ ^5P$ transitions at $10.4\ \mu$ and the $6d\ ^3D \rightarrow 6p\ ^3P$ transitions at $11.7\ \mu$.⁶ The $6d\ ^5D$ and $6p\ ^3P$ states lie respectively $106751\ \text{cm}^{-1}$ and

11. Bates, D.R. (1962) Dielectronic recombination to normal nitrogen and oxygen ions, Planet Space Sci. 9:77.
12. Saum, K.A., and Benesch, W.M. (1970) Infrared electronic emission spectrum of nitrogen, Appl. Opt. 9:195.
13. Saum, K.A., and Benesch, W.M. (1970) Infrared electronic emission spectrum of oxygen, Appl. Opt. 9:1419.

105911 cm^{-1} above the ground state.¹⁰ We might expect the $n = 6$ states to have a slightly lower time-averaged population than the $4d\ ^5D$ state if collisional quenching is important. However, the potential for the $6d\ ^3D$ state giving rise to $11.7\ \mu$ emission must be explored carefully, since this wavelength is in a "window" region of the atmospheric IR background spectrum. Direct observations of LWIR emission from LINUS are planned for the near future.

5. CONCLUSION

We have demonstrated for the first time the capability of observing atomic IR emission from a highly ionized, recombining laser-produced plasma. Time-resolved studies in the visible using an optical multichannel analyzer permit additional detailed studies of the behavior of important atomic IR-emitting states. Future studies include temporal studies of the SWIR emission, which might make possible the observation of weaker lines presently obscured by the time-integrated continuum emission, and extension of these observations into the LWIR.

References

1. Sappenfield, D. (1981) Radiation from a Recombining Oxygen Plasma, Los Alamos Supplemental Report LA-4303.
2. Rawlins, W.T., Gelb, A., and Armstrong, R.A. (1983) COCHISE Observations of Argon Rydberg emission from 2-16 μm , AFGL-TR-83-0201, AD A137916.
3. Murphy, R.W., Fairbairn, A.R., Rogers, W.J., and Hart, A.M. (1975) Near IR nuclear spectra: Interpretation by recent laboratory results, Fourth DARPA Strategic Space Symposium, 23 September 1975.
4. Armstrong, R.A., Lucht, R.A., and Rawlins, W.T. (1983) Spectroscopic investigation of laser-initiated low-pressure plasmas in atmospheric gases, Appl. Opt. 22:1573.
5. Lurie, J.B., and Bashkin, S. to be published.
6. Biemont, E., and Grevesse, N. (1973) Infrared wavelengths and transition probabilities for atoms, $3 \leq Z \leq 20$, Atomic Data and Nuclear Data Tables 12:217.
7. Wiese, W.L., Smith, M.W., and Glennon, B.M. (1966) Atomic Transition Probabilities: Volume I, Hydrogen Through Neon, National Standard Reference Data Series - NBS 4.
8. Bardsley, J.N., and Biondi, M.A. (1970) in Advances in Atomic and Molecular Physics, D.R. Bates (Ed.) Academic, N.Y., Vol. 6, pp. 1-57.
9. Zel'dovich, Ya., and Raizer, Yu. (1966) Physics of Shock Waves and High-Temperature Hydrodynamic Phenomena, Academic Press, N.Y., p. 405.
10. Moore, C.E. (1949) Atomic Energy Levels as Derived from the Analyses of Optical Spectra, NBS Circular 467, 15 June 1949.
11. Bates, D.R. (1962) Dielectronic recombination to normal nitrogen and oxygen ions, Planet Space Sci. 9:77.
12. Saum, K.A., and Benesch, W.M. (1970) Infrared electronic emission spectrum of nitrogen, Appl. Opt. 9:195.
13. Saum, K.A., and Benesch, W.M. (1970) Infrared electronic emission spectrum of oxygen, Appl. Opt. 9:1419.

END

FILMED

2584

DTIC